Diversity of ACE2 and its interaction with SARS-CoV-2 receptor binding domain

Jessie Low-Gan[1,2], Ruiqi Huang[2], Gabrielle Warner[2], Abigail Kelley[2], Duncan McGregor[2], Vaughn Smider[2,3]

[1]San Diego Jewish Academy, San Diego, CA 92130

[2]Applied Biomedical Science Institute, San Diego, CA 92127

[3]The Scripps Research Institute, La Jolla, CA 92037

Correspondence: vaughn.smider@absinstitute.org

Abstract

COVID-19, the clinical syndrome caused by the SARS-CoV-2 virus, has rapidly spread globally causing tens of millions of infections and over a million deaths. The potential animal reservoirs for SARS-CoV-2 are currently unknown, however sequence analysis has provided plausible potential candidate species. SARS-CoV-2 binds to the angiotensin I converting enzyme 2 (ACE2) to enable its entry into host cells and establish infection. We analyzed the binding surface of ACE2 from several important animal species to begin to understand the parameters for the ACE2 recognition by the SARS-CoV-2 spike protein receptor binding domain (RBD). We employed Shannon entropy analysis to determine the variability of ACE2 across its sequence and particularly in its RBD interacting region, and assessed differences between various species' ACE2 and human ACE2. As cattle are a known reservoir for coronaviruses with previous human zoonotic transfer, and has a relatively divergent ACE2 sequence, we compared the binding kinetics of bovine and human ACE2 to SARS-CoV-2 RBD. This revealed a nanomolar binding affinity for bovine ACE2 but an approximate ten-fold reduction of binding compared to human ACE2. Since cows have been experimentally infected by SARS-CoV-2, this lower affinity sets a threshold for sequences with lower homology to human ACE2 to be able to serve as a productive viral receptor for SARS-CoV-2.

32 **Introduction**

33 COVID-19, caused by the novel coronavirus SARS-CoV-2, is a zoonotic disease(1-3) that has thus far
34 resulted in over one million deaths worldwide and over 42 million infections (4). The virus crossed the
35 species boundary, possibly from bats and potentially through an intermediate species, to humans and
36 has spread through the respiratory route across the globe in the past year. SARS-CoV-2 is a member
37 of the betacoronavirus genera, which includes other coronaviruses like SARS-CoV, that caused severe
38 acute respiratory syndrome in a pandemic in 2002-2004 (resulting in approximately 800 deaths in 37
39 countries), and MERS-CoV which caused Middle Eastern Respiratory Syndrome in 2012 (resulting in
40 over 800 deaths in 27 countries). Both of these viruses originated in other species, SARS-CoV in bats,
41 and MERS-CoV in camels, and crossed the species barrier to humans. Other coronaviruses like
42 HCoV-NL63, HCoV-229E, HCoV-HKU1, and HCoV-O43 are known to cause mild respiratory disease in
43 humans and also crossed the species barrier(5-7). Interestingly, the latter two viruses which cause
44 more clinically mild disease appear to have derived from bovine coronavirus (BCoV)(8-10), which
45 causes respiratory and intestinal disease in cattle (7,11-13). Betacoronaviruses as a group have a
46 wide host range including several agricultural and companion animal species(8). Thus, coronavirus
47 disease in humans appears to largely be through zoonotic transfer and has resulted in enormous
48 worldwide morbidity and mortality as well as significant economic loss.

49 Given that coronaviruses appear to have crossed the species barrier several times in human history
50 with devastating consequences, there is a need to understand the interactions between coronaviruses
51 and their receptors in different animal species. This is particularly important since humans interact with
52 companion animals as well as many agricultural species, often in close quarters where respiratory
53 spread can easily occur. In addition to the impact of spread from species to species on human health,
54 coronaviruses can cause devastating effects to animals resulting in morbidity, mortality, and major
55 economic losses (5,7,11,14). Indeed SARS-CoV-2 has been documented to infect dogs (*Canis lupus*),
56 cats (*Felis catus*) (15), and mink (*Mustela lutrola*) (16) in nature, and ferrets (*Mustela putoris)* (15)*,*
57 hamsters (*Cricetulus griseus*) (17) and cows (*Bos taurus*) (18) have been experimentally infected.
58 Human to tiger transfer occurred at the Bronx Zoo (19,20). A mink farm in the Netherlands was
59 ravaged by SARS-CoV-2 infection and farms in the U.S. and Spain were also recently infected (16,21).
60 Additionally, SARS-CoV-2 is now studied *in vivo* in hamsters (*Cricetulus griseus*) and ferrets (*Mustela*
61 *putoris*) as animal models to understand viral pathology and evaluate therapeutics. The need to
62 understand animal susceptibility to coronavirus infection is therefore important to public health, the
63 economy, as well as to establish well understood animal models for therapeutic and vaccine
64 development.

65 SARS-CoV-2 utilizes its trimeric spike protein to bind to the angiotensin I converting enzyme 2 (ACE2)
66 on target pneumocytes or other host cells (22-28). This interaction occurs with high affinity, and results
67 in viral membrane fusion to the host cell and initiates the infectious process. SARS-CoV-1 also utilizes
68 ACE2 as a receptor, however their spike proteins bind with lower affinity (31 nM K_D) than SARS-CoV-2
69 (4.2 nM K_D)(23). Crystal structure and electron microscopy analysis of SARS-CoV-2 with ACE2 has
70 revealed the interacting amino acid residues of the spike receptor binding domain (RBD) and the
71 human ACE2 surface(23,25,29,30). With sequences available for many companion and agriculturally
72 important species, the ability to assess potential spike RBD binding is an important first step towards
73 prediction of infection of these alternative hosts. Here we analyze the conservation and diversity of the
74 ACE2 protein in multiple important animal species, with particular emphasis on the region that interacts
75 with SARS-CoV-2 spike RBD. We confirm that an ACE2 from *Bos taurus*, which is somewhat divergent
76 from human ACE2 in its binding region, interacts with SARS-CoV-2 spike RBD with high affinity,
77 suggesting that multiple mammalian species may be susceptible to infection with this coronavirus.

78

79 **Results**

80 In order to assess the potential of SARS-CoV-2 to interact with ACE2 of important companion and
81 agricultural species, we assembled the ACE2 sequences of several species (Table 1 and Supplemental
82 Table 1). The human ACE2/RBD cocrystal structure (PDB: 6M17)(27) was utilized to visualize
83 interacting residues between the SARS-CoV-2 spike RBD and human ACE2 (Figure 1). In ACE2, 8
84 residues on two helices make direct contact with spike RBD and an additional 17 residues are within 5
85 angstroms of the RBD. These 25 residues are color coded in Figure 1 as purple (contact) and cyan
86 (nearby), respectively. We focused our evaluation on these interacting residues in the following
87 analyses.

88 In order to determine the overall differences between ACE2 of different species, we employed protein
89 sequence alignment as well as variability analysis (Supplemental Figures 1 and 2). All vertebrate
90 ACE2 sequences showed significant homology to human ACE2, with cynomologous and rhesus
91 monkeys being 95% and 94% identical to human (Table 1). Other mammals were between 80-87%
92 identical to human. Horseshoe bats, a potential reservoir for SARS-CoV-2 (28,31) was only 81% and
93 76% identical through the entire sequence and interacting residues, respectively. Surprisingly, the
94 percent identity across the entire ACE2 sequence did not fully correlate with percent identity of the
95 interacting residues. For example, cows show lower homology throughout the entire ACE2 sequence
96 at only 79% compared to the other species, but is 84% identical within the identified interacting

97 residues. In contrast, dogs are 83.3% identical across the entire sequence, but only 76% identical in
98 the interacting residues. A similar lower identity in binding site interacting residues is also seen for
99 rabbits (Table 1). The relative contribution of the interacting residues versus residues outside the RBD
100 binding site is currently not known, although it is expected that the interacting residues are far more
101 important to infection relative to the residues outside of the RBD binding site.

102 For variability analysis, the structural importance of protein regions, and even individual amino acid
103 residues, can be compared across multiple species. Such diversity analyses initially identified the
104 complementary determining regions within antibodies as important interacting domains with antigen by
105 Kabat and Wu(32,33), and more recently Shannon entropy evaluation has been employed to identify
106 conserved and diverse domains of multiple proteins through multiple sequence analysis(34,35). First,
107 we aligned the ACE2 sequences and determined their percent identities (Table 1 and Supplemental
108 Table 1). Then, we calculated Shannon entropy (SE) across the ACE2 sequences. Of note, ACE2 is
109 remarkably conserved across its sequence, with few residues exhibiting high variability (Figure 2).

110 Within the interacting residues, 21 of 25 are highly conserved, with SE values below 2. Significantly, no
111 residues had values above 3. The more variable residues are colored red and conserved residues blue
112 in Figure 2. Five residues, N330, G352, D355, R357, and R393, are completely conserved, with SE
113 values of zero (Figure 2 and Supplemental Table 1). Four of these are nearby residues with RBD, with
114 only R357 being a contact residue. The complete conservation of these residues suggests that they
115 play an important role in the protease function or structural integrity of ACE2. Residues with values
116 between 0 and 1 are K353, which is a contact residue, and L45, Y83, T324, which are nearby residues
117 (Supplemental Table 1). Amino acids with SE values between 1-2 are K26, T27, D30, K31, E35,
118 D38, Q42, M82, and G354. The most diverse residues, with SE values over 2, are Q24, H34, L79, and
119 Q81. Of these, Q24 and H34 are contact residues, with H34 found in a central location in the ACE2-
120 RBD interface (Figure 1, B), and having by far the highest SE value at 2.88 . Others have analyzed the
121 evolution of ACE2 residues and have found positions 24 and 34 to be undergoing positive evolutionary
122 selection pressure (36), and suggested that these positions could play a role in predicting infectivity by
123 SARS-CoV-2 (36).

124 Since the interacting residues are likely most important for viral interaction with ACE2 on the host cell,
125 we evaluated the residues that differed between the various species' ACE2 and human ACE2 in this
126 region (Figure 3 and Supplemental Figure 3). As mentioned, horseshoe bat (*Rhinolophus sinicus*)
127 shares only 19/25 interacting residues (76%) with human ACE2, and only 5/8 contact residues.
128 Specifically, D30E, H34T, Y41H, and M82N (contact residues), and T27M, E35K (nearby residues) are
129 mutated in horseshoe bat ACE2 relative to human ACE2 (Figure 3, upper left), suggesting potentially

130 lower affinity for spike RBD. Pangolin, a possible intermediate host of SARS-CoV-2, has only one
131 contact residue (M82N) and three nearby residues (D38E, L79I, and G354H) altered, and both D38E
132 and L79I are conservative changes (Figure 3, upper right). Felines, which have had documented
133 natural infection (15,20), have only two active site residues mutated (D38E and M82T), and only M82T
134 is a contact residue (Figure 3, middle left). Dogs, which also have been infected naturally, have similar
135 binding site residues as cat but with the notable exception of H34Y (Figure 3, middle), a residue
136 reported to be important in binding. Cow has three interaction site residues mutated, of which M82T is
137 a contact residue, and pig has 5 mutations where Q24L, D30E, H34L, M82T are contact residues
138 (Figure 3 bottom).

139 Cows serve as a reservoir for bovine coronavirus (BCoV) a respiratory infection of cattle that is a
140 betacoronavirus (11,12) distantly related to SARS-CoV-2(7). Of considerable note, two BCoV-related
141 coronaviruses, HCoV-OC43 and HCoV-HKU1, have crossed the species barrier, with OC43 likely from
142 cows to humans to cause “common cold” respiratory disease in humans(37). Whereas BCoV, HCoV-
143 OC43 and HCoV-HKU1 utilize 9-*O*-acetylated sialoglycans as cellular receptors(38), and SARS-CoV-2
144 utilizes ACE2, cows are a potential important species to evaluate for possible SARS-CoV-2 infection as
145 they are a known coronavirus reservoir and they could theoretically serve as host for SARS-CoV-2 and
146 other coronaviruses like BCoV, which could potentially provide a host for coronavirus recombination,
147 selection, and evolution. From a biochemical standpoint, cows have a somewhat more distantly related
148 ACE2 protein compared to many other vertebrates (78.8% compared to most other species which are
149 over 80%), however their binding site residues are more conserved (84%)(Table 1). Therefore, it would
150 be useful to know whether the lower homology across the entire ACE2 sequence prohibits productive
151 ACE2/RBD interaction. To address this question, we expressed human and bovine ACE2 as antibody
152 Fc fusion proteins and compared their interaction with SARS-CoV-2 by enzyme linked immunosorbent
153 assay (ELISA) and further quantified their binding kinetics by surface plasmon resonance analysis
154 (Figure 4). By ELISA, bovine ACE2 had an approximately ten-fold worse binding EC_{50} (0.129 nM for
155 human ACE2 compared to 1.299 nM for bovine ACE2)(Figure 4, A). This lower apparent affinity for
156 bovine ACE2 was confirmed by surface plasmon resonance analysis which showed a K_D for bovine
157 ACE2 of 36.25 nM versus 7.5 nM for human ACE2 (Figure 4, B and Supplementary Table 1). This
158 dissociation constant difference relates primarily to a faster off-rate for bovine ACE2 compared to
159 human ACE2 (Supplementary Figure 5). Of note, despite this lower K_D for bovine ACE2, this affinity is
160 very similar to the K_D for human ACE2 for the RBD of SARS-CoV-1. Interestingly, for both human and
161 bovine ACE2, the SPR data fit more consistently with a two-site model for interaction, suggesting that
162 the RBD may be multimerizing to produce avidity effects on the chip surface. A potential second site
163 would have ten-fold lower K_D values (Supplemental Figure 5), which interestingly, are more in line with

164 the EC_{50} values of the ELISA (Figure 4, A). Such interactions would be important to explore to
165 understand the details of interaction between coronavirus spike RBD and ACE2 on the cell surface.
166 These interactions would be important to inhibit by therapeutic agents, for example by monoclonal
167 antibodies targeting the virus. The avidity interaction may decrease the K_D (increase the affinity) of
168 bovine ACE2 with spike RBD from 36 nM to 2.5 nM, and 7.5 nM to 0.4 nM for human ACE2, a
169 substantial enhancement of the interaction. Regardless of the mechanisms of interaction, it is clear that
170 bovine ACE2 still has high affinity towards SARS-CoV-2 RBD, albeit with five to ten fold worse binding
171 than human ACE2, but yet can still mediate infection of bovine cells(18).

172

173 **Discussion**

174 The recent COVID-19 pandemic has spread rapidly across the globe through human populations, but
175 additionally has also infected several animal species. While zoonotic in origin, it is still unclear which
176 species provided the reservoir for transfer to humans. Coronaviruses as a group have a very wide
177 range of host species, and have jumped the species barrier multiple times to humans(39,40). While
178 bats appear to be a host species for coronaviruses related to SARS-CoV and SARS-CoV-2, it is
179 possible that an as yet unidentified species serves as the reservoir for this virus. Additionally, it is clear
180 that SARS-CoV-2 can naturally infect other species, such as cats, dogs, and mink. In order to
181 understand the host range of SARS-CoV-2 as well as identify potential reservoirs for the virus it is
182 critically important to understand (i) details about the identity and binding properties between the virus
183 and its host cell receptor and possible co-receptors, (ii) other biological requirements needed for the
184 virus to replicate and transmit, for example host cell enzymes needed for viral processing, replication,
185 and assembly. For SARS-CoV-2, ACE2 appears to be the major receptor required for cell entry, so
186 understanding its interaction with ACE2 from humans as well as other species is important to enable
187 predictive methods for viral host range. Here we analyze ACE2 diversity across several species, and
188 specifically evaluate binding of SARS-CoV-2 RBD to bovine ACE2, finding key interacting residues to
189 be highly conserved.

190 Several studies have used sequence homology and/or structural modeling to attempt to predict SARS-
191 CoV-2 RBD binding to various species' ACE2 in order to predict the virus host range(15,36,39-43). In
192 an effort to predict species permissive to infection, Damas et.al. developed a five-tiered scoring scheme
193 based on percent identity of 410 vertebrate species, as well as specific structural features of SARS-
194 CoV-1 or SARS-CoV-2 interactions with ACE2(36). They also focused on 25 amino acid residues at
195 the RBD binding interface, however their 25 residues differed from ours in that they included S16, N53,

196 N90, and N322, with the asparagines included as potential glycosylation sites that may impact RBD
197 binding. However, our approach was agnostic in choosing residues that were either (i) known contact
198 residues with the RBD, or (ii) within 5 angstroms of contact residues. Residues included in our analysis
199 which were not included in Damas et.al. were K26, Q81, and N352. Damas et. al. also note that the
200 host range of SARS-CoV-2 might be quite broad and suggest new species that should be evaluated for
201 animal models of virus infection, which notably include cows, which scored in their "medium" category
202 for predictive binding to RBD. Like our assessment of homology, they find that bats score very low in
203 predicted ACE2 binding. Interestingly, using sequence evolution and selection analysis, they identify
204 Q24 and H34 as positions undergoing positive selection and evolution. We identified these as amongst
205 the most variable residues by Shannon entropy analysis, and these also appear to be important
206 residues at the ACE2/RBD interface. As in our analysis, pangolins scored low in potential RBD binding
207 based on interacting residue homology, suggesting that SARS-CoV-2 may bind other pangolin
208 receptors, or have other mechanisms to interact with ACE2. As pangolins are thought to be a possible
209 intermediate host for SARS-CoV-2, much more biochemical and infectivity data with this controversial
210 species should be obtained.

211 In a different approach, Lam et.al. used structural modeling to predict the change in free energy, $\Delta\Delta G$,
212 for 215 ACE2 sequences derived from different species(44). They correlated the $\Delta\Delta G$ with published
213 infectability information to provide a framework to predict which species may be susceptible to SARS-
214 CoV-2 infection. Like other studies, their work suggests a broad range of mammal susceptibility, with
215 the exception of non-placental mammals. They similarly find that horseshoe bats have higher $\Delta\Delta G$
216 values (*i.e.* lower affinity), calling into question their susceptibility and potential as a reservoir for SARS-
217 CoV-2.

218 There have been several studies that have measured the K_D between SARS-CoV-2 spike (or RBD) and
219 ACE2, with values ranging from 1.2 to 44 nM (23,25,29,30). In these studies, differences in the
220 experimental conditions, such as whether ACE2 or RBD was immobilized, and technique used such as
221 biolayer interferometry versus surface plasmon resonance, could account for differences in kinetic
222 values. In our study, we immobilized ACE2 and measured RBD interaction as the analyte using
223 surface plasmon resonance, which is similar to Lan et. al. who reported a value of K_D = 4.6 nM, which is
224 close to our value of 7.5 nM. However, Lan et.al. as well as all of the other studies utilized a 1:1 model
225 for binding, whereas we found evidence for a two site complexation on the surface, and applied a two
226 site model that gave K_{D1} and K_{D2} values of 7.5 nM and 0.4 nM, respectively. Of considerable note,
227 Forssen et.al. reanalyzed the binding data from Lan et.al. and Tian et.al. and found evidence of
228 multimeric interactions, similar to our study(45). Since the RBD exists in close proximity to two other

229 RBD subunits in the spike protein trimer, it is plausible that cooperative interactions between RBDs
230 exist during ACE2 interaction events. Such events could considerably enhance the interactions
231 providing avidity to enable infection. In this regard, ACE2 variants from species with mutations in the
232 RBD interface may still be permissive to infection because of the cooperative and enhanced avidity of
233 binding events.

234 One of the major challenges in developing predictive methods for viral infectivity is the limited amount
235 of both infection and RBD-ACE2 biochemical interaction data for most species. For example, only few
236 species have had documented infection in the real world, or even in well-controlled experimental
237 systems(15,36,40,44). In this regard, detailed biochemical analysis of multiple species' receptors
238 would provide valuable information that could be used in predictive modeling studies. With the
239 decreased costs of synthetic DNA and high-throughput screening approaches, such analyses could
240 potentially be accomplished rapidly. As a first step in this process, here we evaluate cow ACE2 for
241 binding SARS-CoV-2 RBD by both ELISA and surface plasmon resonance, a species with documented
242 experimental infection by SARS-CoV-2 and of significant agricultural importance that serves as a
243 reservoir for other betacoronaviruses, including at least one, HCoV-O43, that has jumped the species
244 barrier to become an endemic respiratory virus in humans. The affinity of bovine ACE2 is nearly ten-
245 fold worse than human ACE2 in binding the coronavirus RBD, however binding is still in the mid-
246 nanomolar range. Of potential importance is the possible cooperativity in binding that may occur
247 between ACE2 and RBD, which we observed in surface plasmon resonance analysis which suggested
248 a two-site model for binding. Interestingly, this data was consistent with ELISA binding data,
249 suggesting K_D in the subnanomolar range for human, and low nanomolar range for bovine ACE2.
250 Further study into various species' viral receptors, including the recently discovered neuropilin-2 co-
251 receptor for SARS-CoV-2(46), should enable much more accurate and rapid development of predictive
252 algorithms based on viral receptor sequence and structural modelling.

253

254 **Methods**

255 *Sequence and structure analysis*

256 ACE2 sequences from 19 species were obtained from the NCBI protein sequence database. A number
257 of multiple sequence alignments were performed using Clustal Omega. Specific multiple sequence
258 alignments for (i) companion animals (*Canis lupus familiaris, Felis catus, Mus musculus, Mesocricetus*
259 *auratus, Oryctolagus cuniculus*), (ii) agriculturally important animals (*Bos taurus, Capra hircus, Equus*
260 *asinus, Equus caballus, Gallus gallus, Ovis aries, and Sus scrofa*), and (iii) species relevant to animal

261 models or potential reservoirs of interest to vaccine testing research or suspected reservoirs (*Macaca*
262 *mulatta, Macaca fascicularis, Felis catus, Manis javanica, Cricetulus griseus, Canis lupus familiaris,*
263 *Mustela putoris, Sus scrofa, Rhinolophus sinicus, Bos taurus*) were investigated. In all sequence
264 alignments the *Homo sapiens* ACE2 sequence was included as a reference.

265 Further analysis on the multiple sequence alignments were carried out with a variety of software.
266 Phylogenetic trees and pairwise percent identities were obtained with Clustal Omega (47) and
267 visualized in UGENE (http://ugene.net). The open-source EMBL Boxshade Server was used to produce
268 the boxshade alignments (https://embnet.vital-it.ch/software/BOX_form.html). The Protein Variability
269 Server (http://imed.med.ucm.es/PVS/) was employed to calculate Shannon Entropy values for each
270 residue position.

271 For structural analysis, the ACE2 and SARS-CoV-2 Receptor Binding Domain (RBD) complex structure
272 files (PDB) were obtained from the RCSB PDB (PDB ID: 6M17)(27). Eight contact residues of ACE2
273 were identified based on the co-crystal structure (27), and we additionally added 17 ACE2 residues
274 (nearby residues) that were within at least 5 angstroms of the RBD region and classified the full list as
275 "interaction residues". Thus, there were a total of 25 interaction residues, with 8 known RBD contact
276 residues and 17 nearby residues. Using a *de novo* python script, these residues were extracted into a
277 separate "sequence" and an additional, specific multiple sequence alignment was constructed.

278 The interaction residue multiple sequence alignments were investigated to give more focused insight
279 into which species would be at risk of infection, with the assumption that residues directly interacting
280 with the SARS-CoV-2 spike protein would be essential for infection. Structural analyses were
281 performed in Visual Molecular Dynamics (VMD, https://www.ks.uiuc.edu/Research/vmd/).

282 *Protein purification*

283 Human and bovine ACE2 proteins were produced as fusion proteins to human IgG1 Fc according to
284 our published methods for monoclonal antibody purification[2-4]. Briefly, 30 M HEK293 Freestyle cells
285 were transfected with 293fectin combined with 30 µg of pFuse-based vectors containing the human or
286 bovine ACE2 fused to the human Fc region. Cells were shaken at 37 °C for 4 days with 8% CO_2. The
287 media was clarified by centrifugation at 4000 RPM for 5 minutes followed by filtration through a 0.22 µm
288 filter. The media was concentrated and buffer-exchanged into PBS using Amicon Ultra Centrifugal Filter
289 unit (MWCO = 10,000) (MilliporeSigma) at 4 °C. The concentrated media was then loaded onto a
290 protein A-sepharose column (Cytiva) pre-equilibrated with 20 mM sodium phosphate, pH 7.0, followed
291 by washing of the column with 10 column volumes of the same buffer and eluted twice with 1 column
292 volume of 0.1 M glycine-HCl, pH 2.7 into fractions containing 0.1 column volume of 1M Tris, pH 8.

293 Purified proteins were buffer-exchanged into PBS using Amicon Ultra Centrifugal Filter unit (MWCO =
294 10,000) (MilliporeSigma), quantified using 280 nM absorbance on a Nanodrop spectrophotometer
295 (Thermo Fisher Scientific), and resolved on an SDS-PAGE stained with InstantBlue Coomassie Protein
296 Stain (Abcam).

297 The SARS-CoV-2 RBD in plasmid NR-52309 (BEI Resources) was transfected and harvested as
298 described above, but purified using TALON cobalt metal affinity resin (Takara Bio) following the
299 manufacturer's protocol, except that 50 mM, 100 mM, 200 mM and 300 mM imidazole gradient elution
300 fractions (1 column volume of each) were collected. Each elution fraction was resolved on an SDS-
301 PAGE gel stained with InstantBlue Coomassie Protein Stain (Abcam), and fractions containing a single
302 RBD band were pooled, buffer-exchanged into PBS and quantified as described above. Purified
303 protein was resolved on SDS-PAGE with Coomassie (Gel-code blue) staining.

304 *Enzyme linked immunosorbent assay (ELISA)*

305 ELISA plates (Corning 3690) were coated with 100 ng soluble SARS-CoV-2 RBD at 4 ºC in 1 × PBS
306 (pH 7.4) overnight. Plates were washed three times with Tris buffered saline pH 7.4 containing 0.1%
307 Tween-20 (TBST) and blocked with 2% milk (Marvel, dried skim milk dissolved in TBST) at room
308 temperature for 1 h. Serially diluted human or bovine ACE2-Fc were added to the wells in 2%
309 milk/TBST, plates were incubated at room temperature for 1 h, washed four times with TBST and then
310 goat anti-human Fc-HRP (Jackson ImmunoResearch #109-035-098, diluted 1: 5000 in 2% milk/TBST)
311 was added to the wells. Plates were incubated at room temperature for 30 minutes and washed five
312 times with TBST, then developed by adding 50 µl TMB substrate solution (Thermo Scientific) per well
313 and incubated at room temperature for 3 minutes. The HRP-TMB reaction was stopped by adding 50 µl
314 1.0 N sulfuric acid per well. The optical density at 450 nm was read on a microplate reader
315 (SPECTRAMAX M2, Molecular Devices). Antigen-binding curves and EC_{50} values were generated and
316 calculated using four parameter logistic regression in GraphPad Prism 8 (GraphPad Software, Inc., San
317 Diego, CA).

318 *Surface plasmon resonance*

319 Surface plasmon resonance of immobilized ACE2 proteins to RBD as the analyte was performed by
320 Biosensor Tools (https://www.biosensortools.com/ , Salt Lake City, Utah). ACE2-Fc ligands were
321 captured onto a Protein A surface at four different surface densities. Data were collected in Hepes
322 Buffered Saline (HBS) containing 0.1 mg/ml BSA at 25 degrees C. The RBD analyte (36 kDa) was
323 tested in a 3-fold titration series up to 1 uM and 100 nM for both ACE2 protein surfaces at the 4

324 different densities. The data for each data set were fit to a two independent site model. The K_D values
325 indicated in Figure 4 are the average of four experiments at different Rmax values for 100 nM analyte.

326

327

328

329

330 **Table 1. Various species ACE2 percent identity to human ACE2.** The percent identity was
331 calculated across all amino acids of ACE2 (Full length ACE2) or only the interacting residues as shown
332 in Figure 1.

		% Sequence Identity to Human ACE2	
Species		**Full length ACE2**	**Interacting Residues**
Human	*Homo sapiens*	100	100
Cynomolgus monkey	*Macaca fascicularis*	95.03	100
Rhesus monkey	*Macaca mulatta*	94.78	100
Horse	*Equus caball*	86.71	72
Donkey	*Equus asinus*	85.57	72
Cat	*Felis catus*	85.22	80
Rabbit	*Oryctolagus cuniculus*	84.84	76
Pangolin	*Manis javanica*	84.72	68
Golden hamster	*Mesocricetus auratus*	84.47	88
Chinese hamster	*Cricetulus griseus*	84.35	88
Dog	*Canis lupus*	83.33	76
Ferret	*Mustela putorius*	82.48	68
Mouse	*Mus musculus*	82.11	68
Goat	*Capra hircus*	81.72	84
Sheep	*Ovis aries*	81.69	84
Pig	*Sus scrofa*	81.37	76
Bat	*Rhinolophus sinicus*	80.75	72
Cow	*Bos taurus*	78.8	84
Chicken	*Gallus gallus*	66.25	52

333

334

335

336

337

338

339 **Figure Legends**

340 **Figure 1. ACE2 residues interacting with SARS-CoV-2 spike RBD. (A).** The cocrystal structure for
341 the spike RBD (salmon color) and ACE2 (grey, PDB: 6M17) was used to visualize residues that contact
342 the RBD (shaded purple, Q24, D30, H34, Y41, Q42, M82, K353, R357) or are within 5 A of the RBD
343 (shaded cyan, K26, T27, F28, K31, K35, E37, D38, L45, L79, Q81, Y83, T324, N330, G352, G354, ,
344 D355, R393). Throughout the manuscript we refer to these as "contact residues" (purple) and "nearby
345 residues" (cyan), and together as "interacting residues". **(B)** Top down view of ACE2 in space filling
346 mode, with residues color-coded as in (A). G352 is not visible in this orientation. **(C)** Boxshade
347 alignment of only the contact residues and nearby amino acid residues from (B) for multiple species.
348 Contact residues are indicated with a cyan bar on top of the sequence, and nearby residues with a
349 purple bar.

350

351 **Figure 2. Shannon entropy analysis of ACE2 shows low variability. (A)** Shannon entropy plot of
352 the entire ACE2 sequence. The residue positions, and schematic of functional domains are illustrated
353 below the plot. Few residues have values above 2.5, indicating low variability **(B)** (Left) Shannon
354 entropy values projected onto the human ACE2 structure as a heat map from blue (low) to red (high).
355 (Right) View of the RBD-interacting surface as in Figure 1, with contact and nearby residues labeled.
356 Blue residues are very highly conserved.

357

358 **Figure 3. Variable residues at the ACE2-RBD interface of individual species.** With human ACE2
359 as a reference, the variant interacting residues for each species are colored red, and conserved
360 residues colored cyan. For the remainder of the ACE2 protein, conserved residues are white and
361 variable residues light red. Certain residues like M82, Q24, D30, and H34 are often mutated relative to
362 human. D30 is conservatively changed to glutamate, however more non-conservative changes can be
363 seen for H34, for example. More species have been analyzed and are shown in Supplemental Figure
364 3.

365

366 **Figure 4. SARS-CoV-2 spike RBD binds to bovine ACE2 with lower affinity than human ACE2.**
367 **(A)** ELISA of human (red) and bovine (blue) ACE2-Fc binding to immobilized SARS-CoV-2 spike RBD.
368 **(B)** Surface plasmon resonance analysis of RBD as an analyte on immobilized Human ACE-2 Fc (top)
369 or bovine ACE2-Fc (bottom). The data was fit to a two-site model (Supplemental Figure 5). The K_D for
370 site one is indicated, and site two is in parentheses.

371

372 **Supplemental Table 1. Shannon Entropy for RBD interacting residues of ACE2.**

373 **Supplemental Figure 1. Boxshade amino acid sequence alignment of multiple ACE2 species.**

374 **Supplemental Figure 2. Phylogenetic tree of ACE2 from multiple species.**

375 **Supplemental Figure 3. Structures showing variations of the ACE2-RBD interface for four**
376 **species. This analysis was identical to Figure 3.**

377 **Supplemental Figure 4. Pairwise ACE2 percent identities for multiple vertebrate species.**

Supplemental Figure 5. Surface plasmon resonance data for human and bovine ACE2-Fc binding SARS-CoV-2 RBD.

Acknowledgements

The following reagent was produced under HHSN272201400008C and obtained through BEI Resources, NIAID, NIH: Vector pCAGGS Containing the SARS-Related Coronavirus 2, Wuhan-Hu-1 Spike Glycoprotein Receptor Binding Domain (RBD), NR-52309. We thank David Myszka of Biosensor Tools for surface plasmon resonance data analysis.

Author Contributions

JG and VS designed experiments and analyzed data. JG assembled sequences and performed bioinformatic analysis and generated figures. RH designed SARS-CoV-2 RBD expression protocols and purified the RBD protein. GW and AK purified ACE2-Fc proteins and performed ELISA assays and analyzed SPR results. DM and GW designed ACE2 expression vectors. VS and JG wrote the manuscript. VS supervised the project.

Funding

This project was supported in part by National Institutes of Health grant R01 HD088400 to VS.

397 **References**

398 1. Huang, C., Wang, Y., Li, X., Ren, L., Zhao, J., Hu, Y., Zhang, L., Fan, G., Xu, J., Gu, X., Cheng,
399 Z., Yu, T., Xia, J., Wei, Y., Wu, W., Xie, X., Yin, W., Li, H., Liu, M., Xiao, Y., Gao, H., Guo, L.,
400 Xie, J., Wang, G., Jiang, R., Gao, Z., Jin, Q., Wang, J., and Cao, B. (2020) Clinical features of
401 patients infected with 2019 novel coronavirus in Wuhan, China. *Lancet* **395**, 497-506

402 2. Wang, C., Horby, P. W., Hayden, F. G., and Gao, G. F. (2020) A novel coronavirus outbreak of
403 global health concern. *Lancet* **395**, 470-473

404 3. Zhu, N., Zhang, D., Wang, W., Li, X., Yang, B., Song, J., Zhao, X., Huang, B., Shi, W., Lu, R.,
405 Niu, P., Zhan, F., Ma, X., Wang, D., Xu, W., Wu, G., Gao, G. F., Tan, W., China Novel
406 Coronavirus, I., and Research, T. (2020) A Novel Coronavirus from Patients with Pneumonia in
407 China, 2019. *N Engl J Med* **382**, 727-733

408 4. (2020) Johns Hopkins Coronavirus Resource Center.

409 5. Hulswit, R. J. G., de Haan, C. A. M., and Bosch, B. J. (2016) Coronavirus Spike Protein and
410 Tropism Changes. *Adv Virus Res* **96**, 29-57

411 6. Li, F. (2013) Receptor recognition and cross-species infections of SARS coronavirus. *Antiviral*
412 *Res* **100**, 246-254

413 7. Saif, L. J., and Jung, K. (2020) Comparative Pathogenesis of Bovine and Porcine Respiratory
414 Coronaviruses in the Animal Host Species and SARS-CoV-2 in Humans. *J Clin Microbiol* **58**

415 8. Lang, Y., Li, W., Li, Z., Koerhuis, D., van den Burg, A. C. S., Rozemuller, E., Bosch, B. J., van
416 Kuppeveld, F. J. M., Boons, G. J., Huizinga, E. G., van der Schaar, H. M., and de Groot, R. J.
417 (2020) Coronavirus hemagglutinin-esterase and spike proteins coevolve for functional balance
418 and optimal virion avidity. *Proc Natl Acad Sci U S A* **117**, 25759-25770

419 9. Vijgen, L., Keyaerts, E., Lemey, P., Maes, P., Van Reeth, K., Nauwynck, H., Pensaert, M., and
420 Van Ranst, M. (2006) Evolutionary history of the closely related group 2 coronaviruses: porcine
421 hemagglutinating encephalomyelitis virus, bovine coronavirus, and human coronavirus OC43. *J*
422 *Virol* **80**, 7270-7274

423 10. Vijgen, L., Keyaerts, E., Moes, E., Thoelen, I., Wollants, E., Lemey, P., Vandamme, A. M., and
424 Van Ranst, M. (2005) Complete genomic sequence of human coronavirus OC43: molecular
425 clock analysis suggests a relatively recent zoonotic coronavirus transmission event. *J Virol* **79**,
426 1595-1604

427 11. Amer, H. M. (2018) Bovine-like coronaviruses in domestic and wild ruminants. *Anim Health Res*
428 *Rev* **19**, 113-124

429 12. Hodnik, J. J., Jezek, J., and Staric, J. (2020) Coronaviruses in cattle. *Trop Anim Health Prod*

430 13. Saif, L. J. (2010) Bovine respiratory coronavirus. *Vet Clin North Am Food Anim Pract* **26**, 349-
431 364

432 14. Hofmann, H., Simmons, G., Rennekamp, A. J., Chaipan, C., Gramberg, T., Heck, E., Geier, M.,
433 Wegele, A., Marzi, A., Bates, P., and Pohlmann, S. (2006) Highly conserved regions within the
434 spike proteins of human coronaviruses 229E and NL63 determine recognition of their respective
435 cellular receptors. *J Virol* **80**, 8639-8652

436 15. Shi, J., Wen, Z., Zhong, G., Yang, H., Wang, C., Huang, B., Liu, R., He, X., Shuai, L., Sun, Z.,
437 Zhao, Y., Liu, P., Liang, L., Cui, P., Wang, J., Zhang, X., Guan, Y., Tan, W., Wu, G., Chen, H.,
438 and Bu, Z. (2020) Susceptibility of ferrets, cats, dogs, and other domesticated animals to SARS-
439 coronavirus 2. *Science* **368**, 1016-1020

16. Oreshkova, N., Molenaar, R. J., Vreman, S., Harders, F., Oude Munnink, B. B., Hakze-van der Honing, R. W., Gerhards, N., Tolsma, P., Bouwstra, R., Sikkema, R. S., Tacken, M. G., de Rooij, M. M., Weesendorp, E., Engelsma, M. Y., Bruschke, C. J., Smit, L. A., Koopmans, M., van der Poel, W. H., and Stegeman, A. (2020) SARS-CoV-2 infection in farmed minks, the Netherlands, April and May 2020. *Euro Surveill* **25**

17. Rogers, T. F., Zhao, F., Huang, D., Beutler, N., Burns, A., He, W. T., Limbo, O., Smith, C., Song, G., Woehl, J., Yang, L., Abbott, R. K., Callaghan, S., Garcia, E., Hurtado, J., Parren, M., Peng, L., Ramirez, S., Ricketts, J., Ricciardi, M. J., Rawlings, S. A., Wu, N. C., Yuan, M., Smith, D. M., Nemazee, D., Teijaro, J. R., Voss, J. E., Wilson, I. A., Andrabi, R., Briney, B., Landais, E., Sok, D., Jardine, J. G., and Burton, D. R. (2020) Isolation of potent SARS-CoV-2 neutralizing antibodies and protection from disease in a small animal model. *Science*

18. Ulrich, L., Wernike, K., Hoffmann, D., Mettenleiter, T. C., and Beer, M. (2020) Experimental Infection of Cattle with SARS-CoV-2. *Emerg Infect Dis* **26**

19. Ji, W., Wang, W., Zhao, X., Zai, J., and Li, X. (2020) Cross-species transmission of the newly identified coronavirus 2019-nCoV. *J Med Virol* **92**, 433-440

20. Wang, L., Mitchell, P. K., Calle, P. P., Bartlett, S. L., McAloose, D., Killian, M. L., Yuan, F., Fang, Y., Goodman, L. B., Fredrickson, R., Elvinger, F., Terio, K., Franzen, K., Stuber, T., Diel, D. G., and Torchetti, M. K. (2020) Complete Genome Sequence of SARS-CoV-2 in a Tiger from a U.S. Zoological Collection. *Microbiol Resour Announc* **9**

21. Enserink, M. (2020) SARS-CoV-2 infection in farmed minks, the Netherlands, April and May 2020. *Science*

22. Hoffmann, M., Kleine-Weber, H., Schroeder, S., Kruger, N., Herrler, T., Erichsen, S., Schiergens, T. S., Herrler, G., Wu, N. H., Nitsche, A., Muller, M. A., Drosten, C., and Pohlmann, S. (2020) SARS-CoV-2 Cell Entry Depends on ACE2 and TMPRSS2 and Is Blocked by a Clinically Proven Protease Inhibitor. *Cell*

23. Lan, J., Ge, J., Yu, J., Shan, S., Zhou, H., Fan, S., Zhang, Q., Shi, X., Wang, Q., Zhang, L., and Wang, X. (2020) Structure of the SARS-CoV-2 spike receptor-binding domain bound to the ACE2 receptor. *Nature*

24. Letko, M., Marzi, A., and Munster, V. (2020) Functional assessment of cell entry and receptor usage for SARS-CoV-2 and other lineage B betacoronaviruses. *Nat Microbiol* **5**, 562-569

25. Walls, A. C., Park, Y. J., Tortorici, M. A., Wall, A., McGuire, A. T., and Veesler, D. (2020) Structure, Function, and Antigenicity of the SARS-CoV-2 Spike Glycoprotein. *Cell*

26. Wang, Q., Zhang, Y., Wu, L., Niu, S., Song, C., Zhang, Z., Lu, G., Qiao, C., Hu, Y., Yuen, K. Y., Wang, Q., Zhou, H., Yan, J., and Qi, J. (2020) Structural and Functional Basis of SARS-CoV-2 Entry by Using Human ACE2. *Cell*

27. Yan, R., Zhang, Y., Li, Y., Xia, L., Guo, Y., and Zhou, Q. (2020) Structural basis for the recognition of SARS-CoV-2 by full-length human ACE2. *Science* **367**, 1444-1448

28. Zhou, P., Yang, X. L., Wang, X. G., Hu, B., Zhang, L., Zhang, W., Si, H. R., Zhu, Y., Li, B., Huang, C. L., Chen, H. D., Chen, J., Luo, Y., Guo, H., Jiang, R. D., Liu, M. Q., Chen, Y., Shen, X. R., Wang, X., Zheng, X. S., Zhao, K., Chen, Q. J., Deng, F., Liu, L. L., Yan, B., Zhan, F. X., Wang, Y. Y., Xiao, G. F., and Shi, Z. L. (2020) A pneumonia outbreak associated with a new coronavirus of probable bat origin. *Nature* **579**, 270-273

29. Shang, J., Ye, G., Shi, K., Wan, Y., Luo, C., Aihara, H., Geng, Q., Auerbach, A., and Li, F. (2020) Structural basis of receptor recognition by SARS-CoV-2. *Nature* **581**, 221-224

484 30. Wrapp, D., Wang, N., Corbett, K. S., Goldsmith, J. A., Hsieh, C. L., Abiona, O., Graham, B. S.,
485 and McLellan, J. S. (2020) Cryo-EM structure of the 2019-nCoV spike in the prefusion
486 conformation. *Science* **367**, 1260-1263

487 31. Zhou, J., Li, C., Liu, X., Chiu, M. C., Zhao, X., Wang, D., Wei, Y., Lee, A., Zhang, A. J., Chu, H.,
488 Cai, J. P., Yip, C. C., Chan, I. H., Wong, K. K., Tsang, O. T., Chan, K. H., Chan, J. F., To, K. K.,
489 Chen, H., and Yuen, K. Y. (2020) Infection of bat and human intestinal organoids by SARS-
490 CoV-2. *Nat Med* **26**, 1077-1083

491 32. Kabat, E. A., and Wu, T. T. (1991) Identical V region amino acid sequences and segments of
492 sequences in antibodies of different specificities. Relative contributions of VH and VL genes,
493 minigenes, and complementarity-determining regions to binding of antibody-combining sites. *J*
494 *Immunol* **147**, 1709-1719

495 33. Wu, T. T., and Kabat, E. A. (1970) An analysis of the sequences of the variable regions of
496 Bence Jones proteins and myeloma light chains and their implications for antibody
497 complementarity. *J. Exp. Med.* **132**, 211-250

498 34. Deiss, T. C., Vadnais, M., Wang, F., Chen, P. L., Torkamani, A., Mwangi, W., Lefranc, M.-P.,
499 Criscitiello, M. F., and Smider, V. V. (2017) Immunogenetic factors driving formation of ultralong
500 VH CDR3 in Bos taurus antibodies. *Cell Mol Immunol* **14**, 1-12

501 35. Strait, B. J., and Dewey, T. G. (1996) The Shannon information entropy of protein sequences.
502 *Biophys J* **71**, 148-155

503 36. Damas, J., Hughes, G. M., Keough, K. C., Painter, C. A., Persky, N. S., Corbo, M., Hiller, M.,
504 Koepfli, K. P., Pfenning, A. R., Zhao, H., Genereux, D. P., Swofford, R., Pollard, K. S., Ryder, O.
505 A., Nweeia, M. T., Lindblad-Toh, K., Teeling, E. C., Karlsson, E. K., and Lewin, H. A. (2020)
506 Broad host range of SARS-CoV-2 predicted by comparative and structural analysis of ACE2 in
507 vertebrates. *Proc Natl Acad Sci U S A* **117**, 22311-22322

508 37. Cui, J., Li, F., and Shi, Z. L. (2019) Origin and evolution of pathogenic coronaviruses. *Nat Rev*
509 *Microbiol* **17**, 181-192

510 38. Hulswit, R. J. G., Lang, Y., Bakkers, M. J. G., Li, W., Li, Z., Schouten, A., Ophorst, B., van
511 Kuppeveld, F. J. M., Boons, G. J., Bosch, B. J., Huizinga, E. G., and de Groot, R. J. (2019)
512 Human coronaviruses OC43 and HKU1 bind to 9-O-acetylated sialic acids via a conserved
513 receptor-binding site in spike protein domain A. *Proc Natl Acad Sci U S A* **116**, 2681-2690

514 39. Mathavarajah, S., and Dellaire, G. (2020) Lions, tigers and kittens too: ACE2 and susceptibility
515 to COVID-19. *Evol Med Public Health* **2020**, 109-113

516 40. Salajegheh Tazerji, S., Magalhaes Duarte, P., Rahimi, P., Shahabinejad, F., Dhakal, S., Singh
517 Malik, Y., Shehata, A. A., Lama, J., Klein, J., Safdar, M., Rahman, M. T., Filipiak, K. J.,
518 Rodriguez-Morales, A. J., Sobur, M. A., Kabir, F., Vazir, B., Mboera, L., Caporale, M., Islam, M.
519 S., Amuasi, J. H., Gharieb, R., Roncada, P., Musaad, S., Tilocca, B., Koohi, M. K., Taghipour,
520 A., Sait, A., Subbaram, K., Jahandideh, A., Mortazavi, P., Abedini, M. A., Hokey, D. A., Hogan,
521 U., Shaheen, M. N. F., Elaswad, A., Elhaig, M. M., and Fawzy, M. (2020) Transmission of
522 severe acute respiratory syndrome coronavirus 2 (SARS-CoV-2) to animals: an updated review.
523 *J Transl Med* **18**, 358

524 41. Hayashi, T., Abiko, K., Mandai, M., Yaegashi, N., and Konishi, I. (2020) Highly conserved
525 binding region of ACE2 as a receptor for SARS-CoV-2 between humans and mammals. *The*
526 *veterinary quarterly* **40**, 243-249

527 42. Lam, T. T., Jia, N., Zhang, Y. W., Shum, M. H., Jiang, J. F., Zhu, H. C., Tong, Y. G., Shi, Y. X.,
528 Ni, X. B., Liao, Y. S., Li, W. J., Jiang, B. G., Wei, W., Yuan, T. T., Zheng, K., Cui, X. M., Li, J.,

529 Pei, G. Q., Qiang, X., Cheung, W. Y., Li, L. F., Sun, F. F., Qin, S., Huang, J. C., Leung, G. M.,
530 Holmes, E. C., Hu, Y. L., Guan, Y., and Cao, W. C. (2020) Identifying SARS-CoV-2-related
531 coronaviruses in Malayan pangolins. *Nature* **583**, 282-285

532 43. Qiu, Y., Zhao, Y. B., Wang, Q., Li, J. Y., Zhou, Z. J., Liao, C. H., and Ge, X. Y. (2020) Predicting
533 the angiotensin converting enzyme 2 (ACE2) utilizing capability as the receptor of SARS-CoV-2.
534 *Microbes Infect* **22**, 221-225

535 44. Lam, S. D., Bordin, N., Waman, V. P., Scholes, H. M., Ashford, P., Sen, N., van Dorp, L., Rauer,
536 C., Dawson, N. L., Pang, C. S. M., Abbasian, M., Sillitoe, I., Edwards, S. J. L., Fraternali, F.,
537 Lees, J. G., Santini, J. M., and Orengo, C. A. (2020) SARS-CoV-2 spike protein predicted to
538 form complexes with host receptor protein orthologues from a broad range of mammals. *Sci*
539 *Rep* **10**, 16471

540 45. Forssen, P., Samuelsson, J., Lacki, K., and Fornstedt, T. (2020) Advanced Analysis of
541 Biosensor Data for SARS-CoV-2 RBD and ACE2 Interactions. *Anal Chem* **92**, 11520-11524

542 46. Daly, J. L., Simonetti, B., Klein, K., Chen, K.-E., Williamson, M. K., Antón-Plágaro, C.,
543 Shoemark, D. K., Simón-Gracia, L., Bauer, M., Hollandi, R., Greber, U. F., Horvath, P.,
544 Sessions, R. B., Helenius, A., Hiscox, J. A., Teesalu, T., Matthews, D. A., Davidson, A. D.,
545 Collins, B. M., Cullen, P. J., and Yamauchi, Y. (2020) Neuropilin-1 is a host factor for SARS-
546 CoV-2 infection. *Science*, eabd3072

547 47. Madeira, F., Park, Y. M., Lee, J., Buso, N., Gur, T., Madhusoodanan, N., Basutkar, P., Tivey, A.
548 R. N., Potter, S. C., Finn, R. D., and Lopez, R. (2019) The EMBL-EBI search and sequence
549 analysis tools APIs in 2019. *Nucleic Acids Res* **47**, W636-W641

550

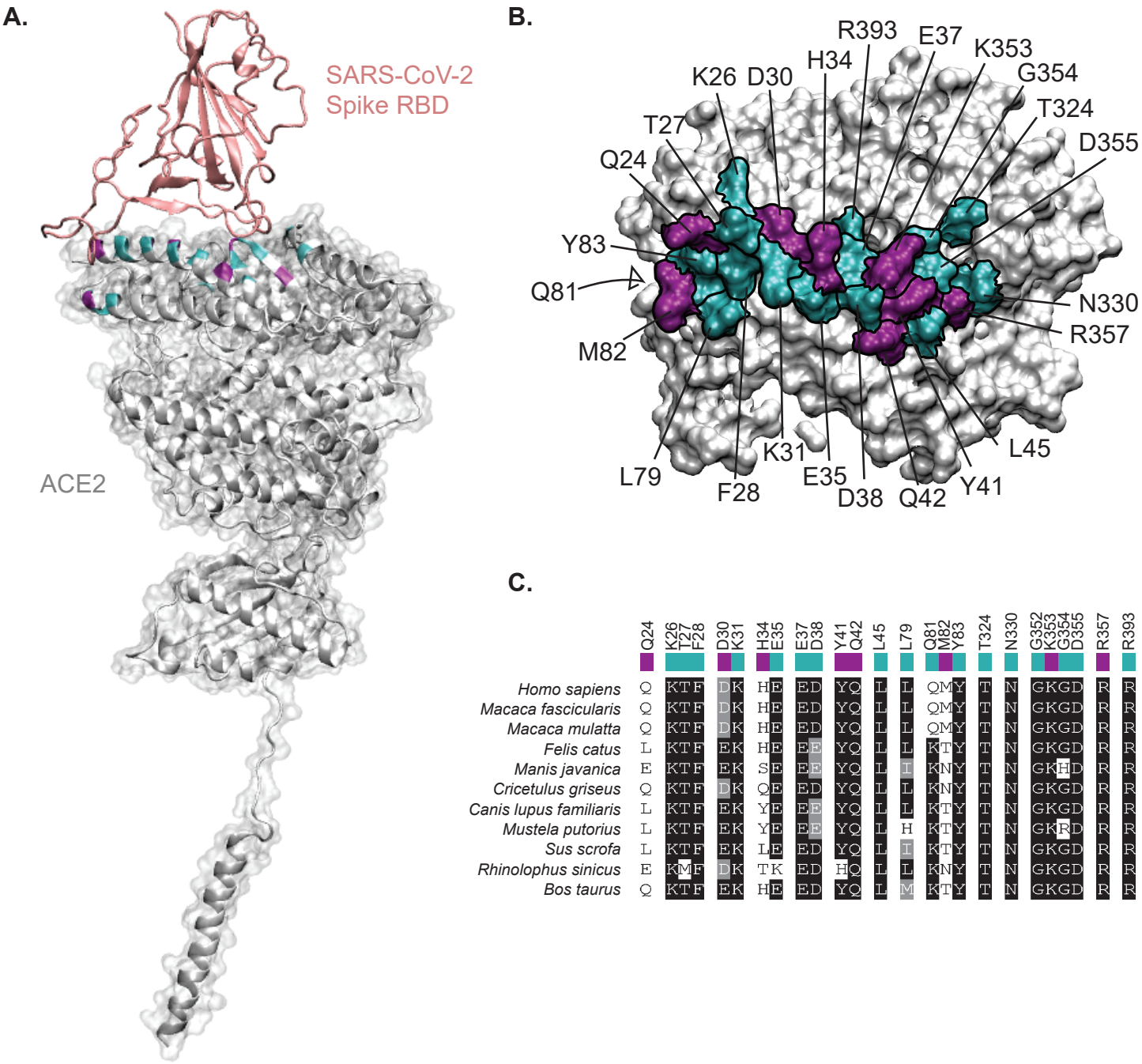
A.
SARS-CoV-2
Spike RBD
ACE2
B.
R393
E37
K353
H34
G354
K26
D30
T324
T27
D355
Q24
Y83
Q81
N330
R357
M82
L45
K31
L79
E35
Y41
F28
D38
Q42
C.
Q24
K26 T27 F28
D30 K31
H34 E35
E37 D38
Y41 Q42
L45
L79
Q81 M82 Y83
T324
N330
G352 K353 G354 D355
R357
R393
Homo sapiens Q KTF DK HE ED YQ L L QMY T N GKGD R R
Macaca fascicularis Q KTF DK HE ED YQ L L QMY T N GKGD R R
Macaca mulatta Q KTF DK HE ED YQ L L QMY T N GKGD R R
Felis catus L KTF EK HE EE YQ L L KTY T N GKGD R R
Manis javanica E KTF EK SE EE YQ L I KNY T N GKHD R R
Cricetulus griseus Q KTF DK QE ED YQ L L KNY T N GKGD R R
Canis lupus familiaris L KTF EK YE EE YQ L L KTY T N GKGD R R
Mustela putorius L KTF EK YE EE YQ L H KTY T N GKRD R R
Sus scrofa L KTF EK LE ED YQ L I KTY T N GKGD R R
Rhinolophus sinicus E KMF DK TK ED HQ L L KNY T N GKGD R R
Bos taurus Q KTF EK HE ED YQ L M KTY T N GKGD R R

Figure 1

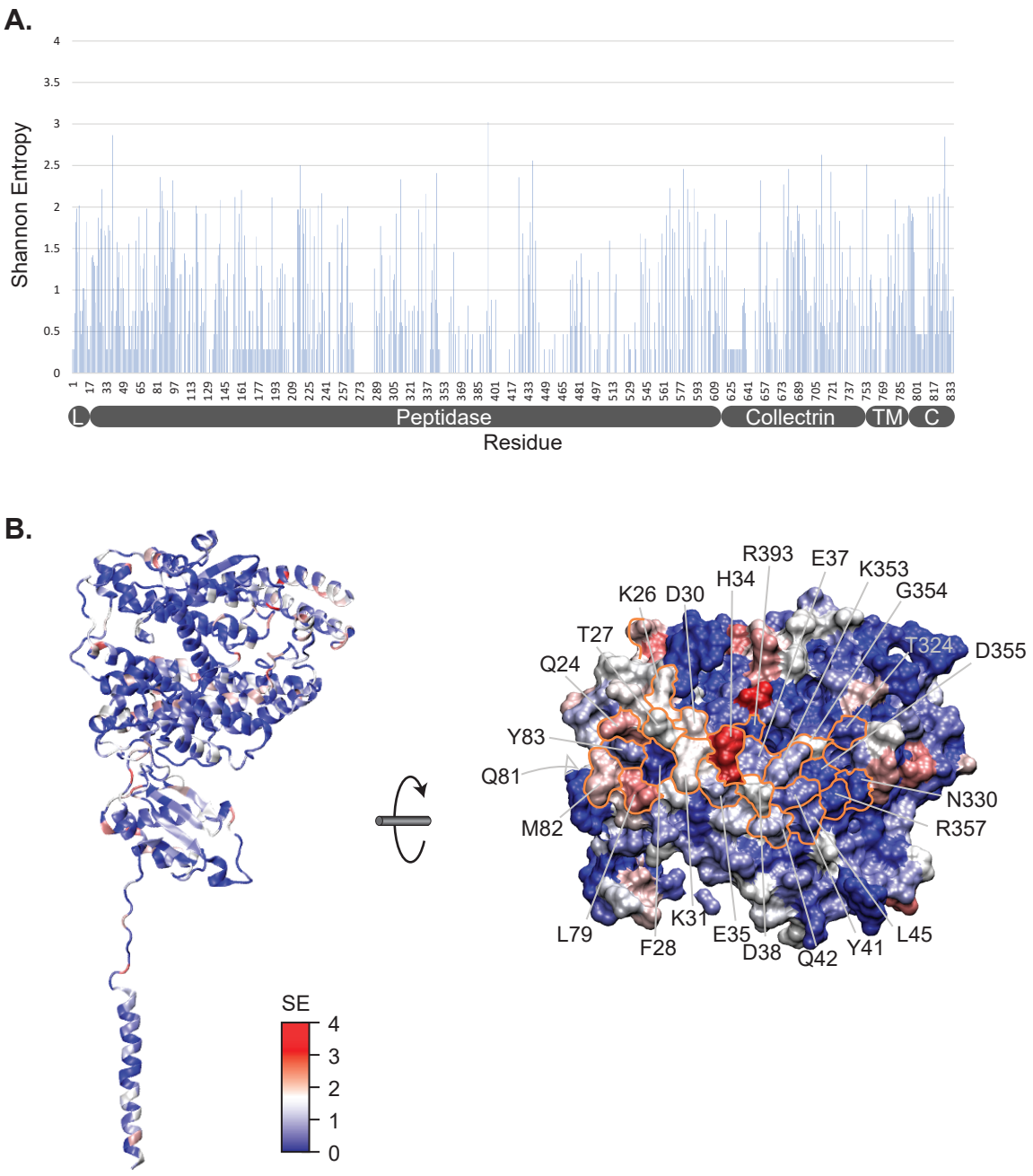
A.
Shannon Entropy
Residue
L
Peptidase
Collectrin
TM
C
B.
SE
4
3
2
1
0
R393
E37
K353
H34
K26
D30
G354
T27
T324
D355
Q24
Y83
Q81
N330
M82
R357
K31
L79
E35
L45
F28
D38
Y41
Q42

Figure 2

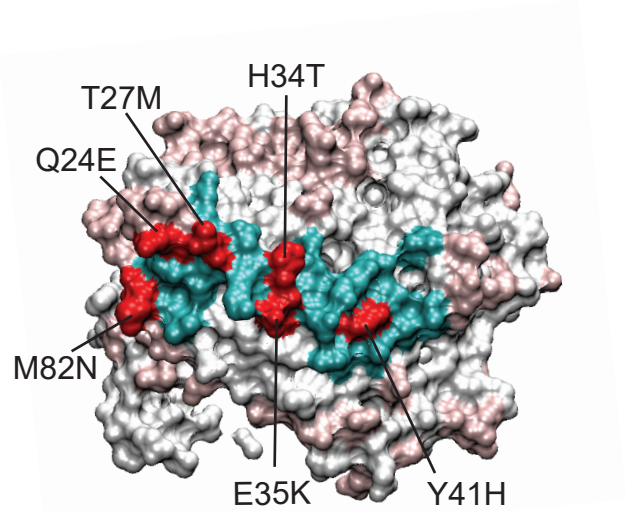

Rhinolophus sinicus (horseshoe bat)

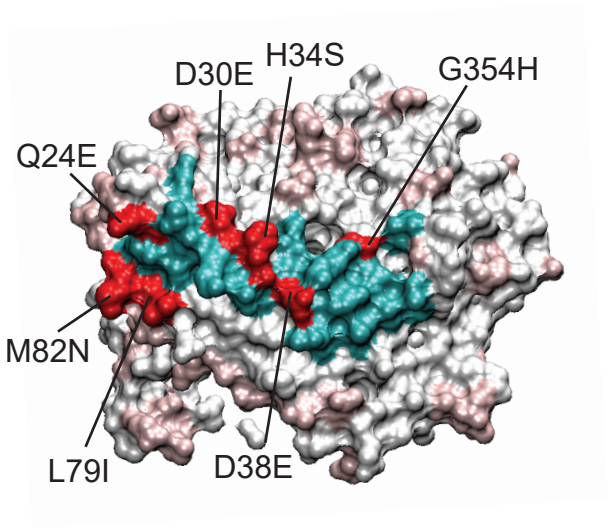

Manis javanica (pangolin)

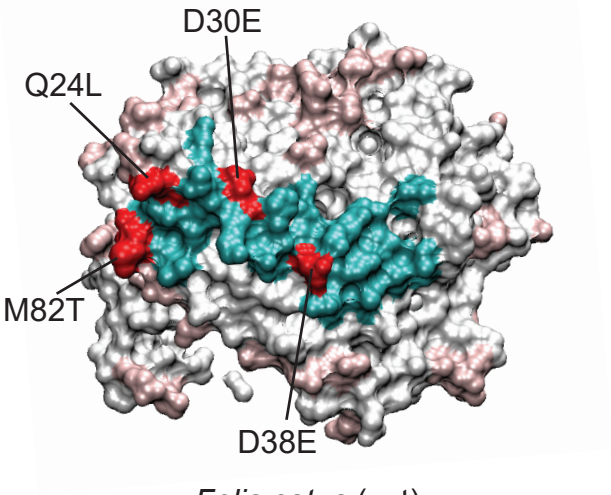

Felis catus (cat)

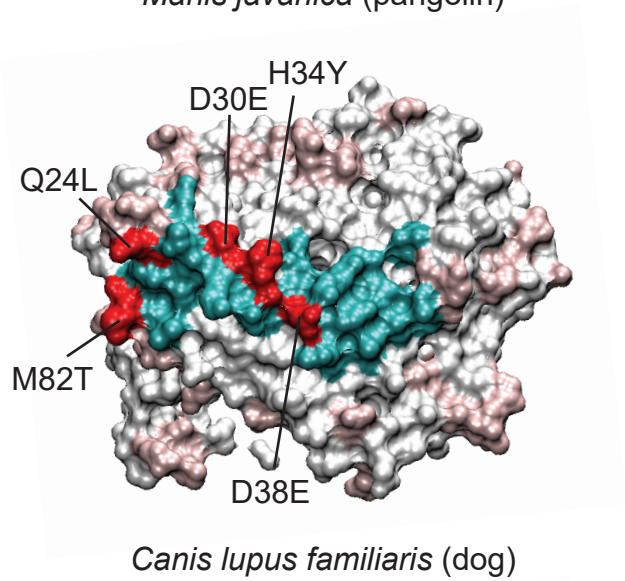

Canis lupus familiaris (dog)

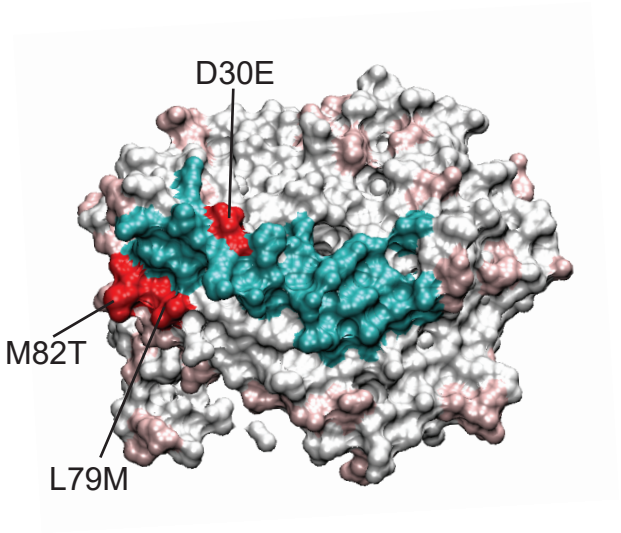

Bos taurus (cow)

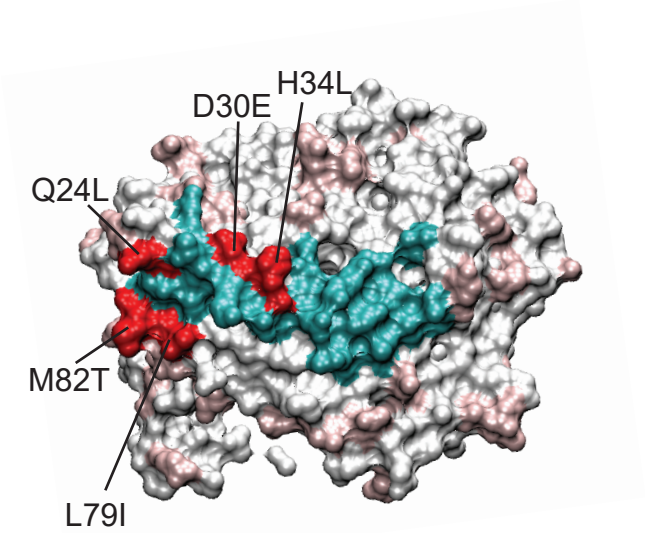

Sus scrofa (pig)

Figure 3

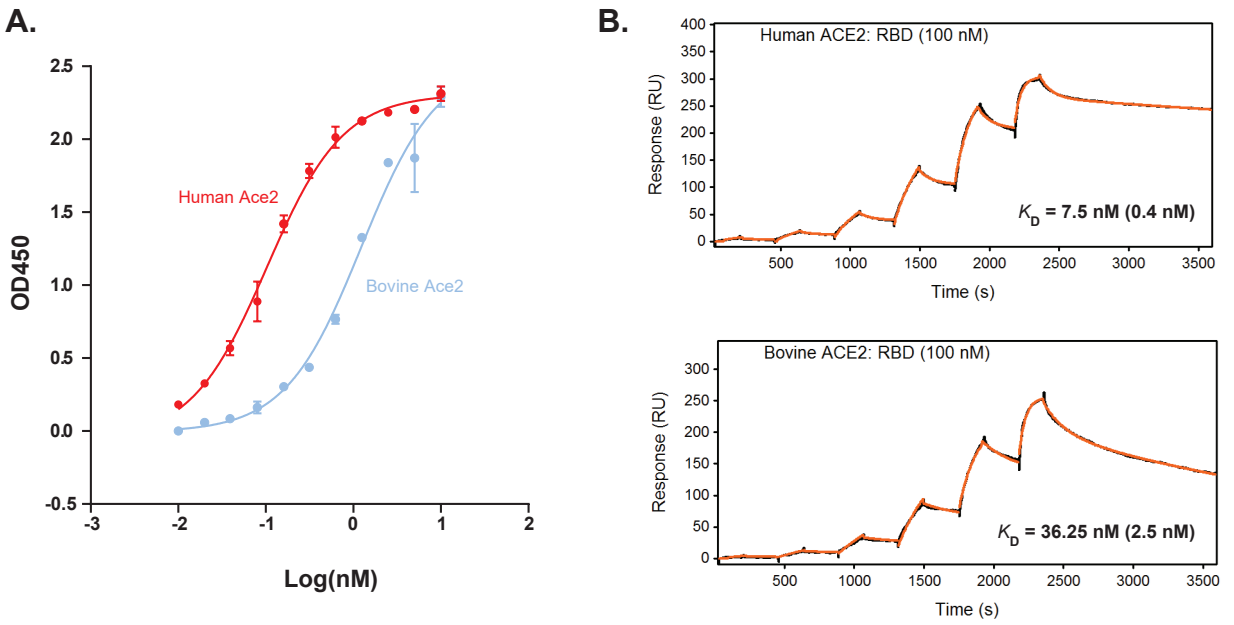
A.
OD450
Log(nM)
Human Ace2
Bovine Ace2
B.
Human ACE2: RBD (100 nM)
Response (RU)
Time (s)
K_D = 7.5 nM (0.4 nM)
Bovine ACE2: RBD (100 nM)
Response (RU)
Time (s)
K_D = 36.25 nM (2.5 nM)

Figure 4